

Impact of nuclear deformation on longitudinal flow decorrelations in high-energy isobar collisions

Maowu Nie,^{1,2} Chunjian Zhang,³ Zhenyu Chen,^{1,2} Li Yi,^{1,2} and Jiangyong Jia^{3,4}

¹*Institute of Frontier and Interdisciplinary Science,
Shandong University, Qingdao, 266237, China*

²*Key Laboratory of Particle Physics and Particle Irradiation,
Ministry of Education, Shandong University, Qingdao, Shandong, 266237, China*

³*Department of Chemistry, Stony Brook University, Stony Brook, New York 11794, USA*

⁴*Physics Department, Brookhaven National Laboratory, Upton, New York 11976, USA*

Fluctuations of harmonic flow along pseudorapidity η , known as flow decorrelations, is an important probe of the initial condition and final state evolution of the quark-gluon plasma. We show that the flow decorrelations are sensitive to the deformations of the colliding nuclei. This sensitivity is revealed clearly by comparing flow decorrelations between collisions of isobars, $^{96}\text{Zr}+^{96}\text{Zr}$ and $^{96}\text{Ru}+^{96}\text{Ru}$, which have different deformations. Longitudinal flow decorrelations in heavy-ion collisions is a new tool to probe the structure of colliding nuclei.

PACS numbers:

I. INTRODUCTION

Azimuthal anisotropic flow [1] is an important tool to study the properties of the quark-gluon plasma produced in high-energy heavy-ion collisions at Relativistic Heavy Ion Collider (RHIC) and the Large Hadron Collider (LHC) [2–4]. The flow is characterized via a Fourier expansion of particle production $dN/d\phi \propto 1 + 2\sum_{n=1}^{\infty} v_n \cos n(\phi - \Psi_n)$, where v_n and Ψ_n are the n^{th} -order of flow magnitude and phase, respectively. The dominating components v_2 (elliptic flow) [5] and v_3 (triangular flow) [6] have been studied extensively. They have led to constraints on both the initial condition as well as the transport properties of the QGP [7–9].

One important insight realized recently is that the heavy-ion initial condition is not boost invariant in the longitudinal direction. In fact, it interpolates between projectile nucleus geometry in the forward direction and target nucleus geometry in the backward direction. These two geometries are not the same due to random fluctuations of participating nucleons, which leads to a twist in the final state event-plane angles [10–14]. This effects have been measured at both the LHC [15–17] and RHIC [18], and are well described by 3+1D event-by-event viscous hydrodynamical models [19–25, 25]. The experimental observable for flow decorrelation is constructed from ratios of two-particle correlations

$$r_n(\eta, \eta_{\text{ref}}) = \frac{V_{n\Delta}(-\eta, \eta_{\text{ref}})}{V_{n\Delta}(\eta, \eta_{\text{ref}})} \quad (1)$$

where the η_{ref} is the reference pseudorapidity common to the numerator and the denominator, typically chosen at forward rapidity. The decorrelation is reflected by the fact that $V_{n\Delta}(\eta, \eta_{\text{ref}}) \neq v_n(\eta)v_n(\eta_{\text{ref}})$, and appearing as a linear decrease

of r_n as a function of η .

The longitudinal fluctuations of the initial condition are strongly influenced by the collective structure of the colliding nuclei [26, 27]. Most heavy nuclei are more or less deformed from spherical shape and can be described by a Woods-Saxon form:

$$\rho(r, \theta, \phi) = \frac{\rho_0}{1 + e^{(r-R(\theta, \phi))/a}} \quad (2)$$

$$R(\theta, \phi) = R_0(1 + \beta_2 Y_2^0 + \beta_3 Y_3^0) \quad (3)$$

where the nuclear surface $R(\theta, \phi)$ includes quadrupole deformation β_2 and octupole deformation β_3 . R_0 and a are the half-height radius and nuclear skin, respectively. Recent studies show that the v_n are strongly enhanced by β_n , especially in the ultra-central collisions. The v_n are also influenced by the R_0 and a in the mid-central collisions [28]. The evidence for these influences is best revealed by ratios of v_n between two isobar collision systems with different structures. Since isobar nuclei have the same mass number but different structures, deviation from the unity of the ratio of any observable must originate from differences in the structure of the colliding nuclei, which impact the initial state of QGP and its final state evolution. One such example is the $^{96}\text{Zr}+^{96}\text{Zr}$ and $^{96}\text{Ru}+^{96}\text{Ru}$ collisions, which have shown significant departure from unity in the ratios of many observables, including v_2 and v_3 [29]. The structure differences between ^{96}Ru and ^{96}Zr are also expected to cause differences in the longitudinal structure of the initial condition and subsequently the flow decorrelations.

This paper studies the influence of nuclear deformation β_2 and β_3 on the flow decorrelations $^{96}\text{Zr}+^{96}\text{Zr}$ and $^{96}\text{Ru}+^{96}\text{Ru}$ collisions within a Multi-phase transport model (AMPT). We focus in particular on the ratios of the r_n between

the two systems, which show significant deviation from unity in the presence of deformations.

II. THE AMPT MODEL

In AMPT model, the initial partons can be treated as strings in the longitudinal direction, with the fluctuation of the length of the strings, longitudinal fluctuation was naturally introduced, previous studies suggest it can well describe the flow decorrelation in heavy-ion collisions [30, 31]. We use the AMPT string melting version to simulate isobar $^{96}\text{Zr}+^{96}\text{Zr}$ and $^{96}\text{Ru}+^{96}\text{Ru}$ collisions at $\sqrt{s_{\text{NN}}} = 200$ GeV. The string melting version consists of four main components: Monte Carlo Glauber as initial conditions, strings and mini-jet that melt into partons from the HIJING model [32], elastic parton cascade by the ZPC model [33], a quark coalescence model for hadronization, and hadron rescatterings described by the ART model [34]. For details, see the review [35].

The Wood-Saxon parameters for the two collision systems are set with $R_0 = 5.09$ fm and $a = 0.52$ fm, the deformation parameter is set with $\beta_2 = 0.162$ and $\beta_3 = 0$ for Ru, $\beta_2 = 0.06$ and $\beta_3 = 0.2$ for Zr. The elastic parton-parton cross section is $\sigma = 3$ mb, which is also used in recent AMPT studies [36, 37].

Recent studies also suggest the neutron skin and the symmetry energy are different between $^{96}\text{Zr}+^{96}\text{Zr}$ and $^{96}\text{Ru}+^{96}\text{Ru}$ collisions [38, 39], for simplicity, these effects are not included in this study.

III. RESULTS AND DISCUSSIONS

The major difference between Zr+Zr and Ru+Ru in this study is the initial deformation, thus any differences in the final observable ratios between the two collision systems will directly reflect the nuclear structure. The isobar ratio is also studied in a recent study, which suggests the final state observable isobar ratio is insensitive to the final state effects, such as the shear viscosity, hadronization, and hadronic cascade [40]. Fig. 1 show r_2 and r_3 as a function of η averaged over $0.4 < p_T < 4$ GeV for Zr+Zr and Ru+Ru collisions in two centrality intervals 0-10% and 10-40%, where reference pseudorapidity ranges are $3.1 < |\eta_{\text{ref}}| < 5.1$ for r_2 and $2.1 < |\eta_{\text{ref}}| < 5.1$ for r_3 . The contributions from nonflow like dijets are expected to contribute to r_2 due to the small gap between η and η_{ref} . $3.1 < |\eta_{\text{ref}}| < 5.1$ can significantly suppress these non-flow contributions, while r_3 is almost independent of reference rapidity ranges, $2.1 < |\eta_{\text{ref}}| < 5.1$ enables us have

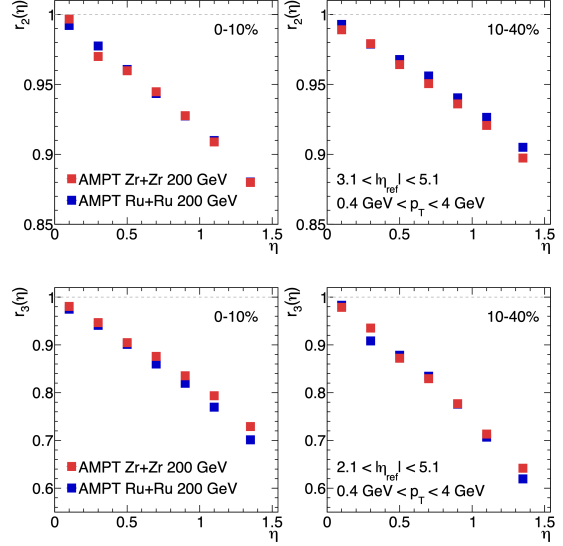


Figure 1: r_2 (top) and r_3 (bottom) as a function of pseudorapidity η in Zr+Zr and Ru+Ru collisions in 0-10% and 10-40% centralities.

sufficient statistics for r_3 in this study. Though Ru+Ru collisions show a similar trend as Zr+Zr collisions, the differences of r_2 and r_3 between the two collision systems are still clear. For r_2 , the difference for most central collision 0-10% is negligible, while 10-40% shows a clear difference, especially at large pseudorapidity. However for r_3 , both 0-10% and 10-40% show clear deviation. It is worth noticing that the recent STAR preliminary results show the a similar trend [41].

To further quantify the difference, the ratio between Ru+Ru and Zr+Zr is analytically calculated in Fig. 2. r_2 ratio is consistent with 1 within error in 0-10%, while it shows a clear difference for 10-40%, and the difference is up to 1%. Previous study suggest the presence of $\beta_{3,Zr}$ can significantly enhance $v_{2,Zr}$ in mid-central collisions [37], it could be the same reason on the negligible difference in r_2 ratio in 0-10%. Unlike r_2 ratio, the r_3 ratio is significantly less than 1, the difference can go up to 4% in both 0-10% and 10-40%. The results suggest r_n is also sensitive to the nuclear structure, and r_n ratio can provide a more direct way to quantify the difference, which can be used in future experimental measurements.

The factorization ratio r_n can be parametrized with a linear function: $r_n(\eta) = 1 - 2F_n\eta$, where slope parameter F_n quantified the strength of flow decorrelation. Thus F_n can be well extracted for each centrality interval. To better quantify the centrality dependence of F_n , the centrality bins are redefined with 10% interval. As in ultra-central collisions, the initial geometry will involve more nuclear deformation effect, we further ex-

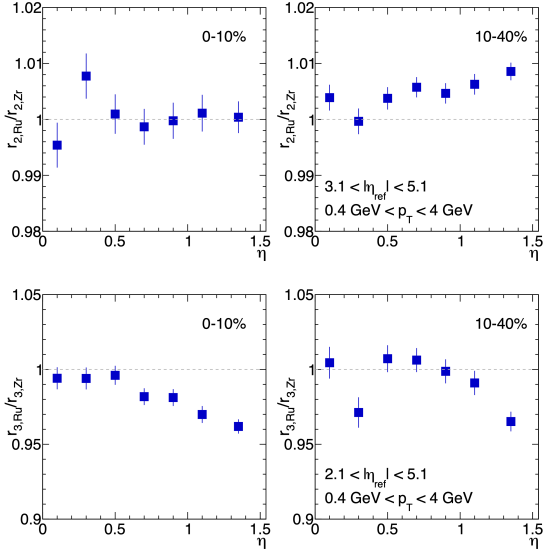


Figure 2: Ratio of r_2 (top) and r_3 (bottom) between Zr+Zr and Ru+Ru collisions in 0-10% and 10-40% centralities.

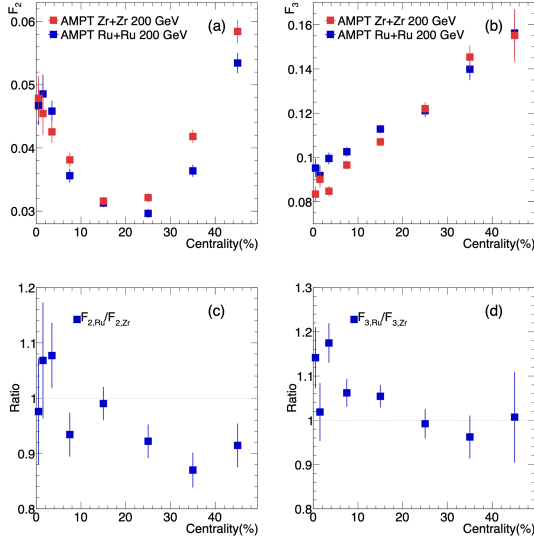


Figure 3: Centrality dependence of slope parameter F_2 (left) and F_3 (right) in Zr+Zr and Ru+Ru collisions.

tend the 0-10% to finer bins: 0-1%, 1-2%, 2-5%, and 5-10%. For each centrality interval the F_2 and F_3 are obtained via a linear regression coefficients with $F_n = \frac{\sum_i 1-r_n(\eta_i)\eta_i}{2\sum_i \eta_i^2}$, where n denotes the harmonic and the sum runs over all data points. Fig 3 (a) and (b) show F_2 and F_3 as a function of centrality of the two collisions systems. Clear centrality dependence is observed for F_2 in both systems, where decorrelation is stronger in central and peripheral collisions. Such behav-

ior is strongly correlated with v_2 , where the average elliptic geometry is strongest in mid-central collisions, which leads to the weakest longitudinal fluctuation. As we know, v_3 is fluctuation driven and is almost independent of centrality. F_3 shows slightly centrality dependence, where F_3 is increasing with larger centrality bins, which may attribute to a stronger longitudinal fluctuation in peripheral collisions. Fig 3 (a) and (b) also show a larger F_2 in peripheral collisions for the Zr+Zr system, and a larger F_3 in most central collisions for the Ru+Ru system.

Fig. 3 (c) and (d) compared the centrality dependence of the ratios of slope parameters F_2 and F_3 between Ru+Ru and Zr+Zr systems. The F_n difference can be quantified with F_n ratio between the two systems. F_2 ratio is almost consistent with 1 in central collisions, and it shows up to 10% difference in mid-central collisions, while for F_3 ratio, the difference is large in central and becomes consistent with 1 in mid-central collisions. Since a large quadrupole deformation β_2 is implemented in Ru+Ru collisions, and a large octupole deformation β_3 for Zr+Zr collisions, the difference of F_2 and F_3 between the two collision systems directly reflect the nuclear structure difference.

IV. CONCLUSION

The impact of nuclear deformation on longitudinal flow decorrelation in Zr+Zr and Ru+Ru collisions is studied in AMPT string melting framework. With a large quadrupole deformation of Ru and large octupole deformation of Zr, clear differences in flow decorrelations are observed between the two collision systems. We further propose r_n ratio to quantify the differences between the two systems, and the deviation can go up to 1% for r_2 in 10-40% and 5% for r_3 in 0-10% at large η . The slow parameter F_n of r_n are studied as a function of centrality. Around 10% difference is observed for F_2 in mid-central collisions, and up to 20% difference for F_3 in most central collisions. The results suggest the longitudinal dynamics are also sensitive to the nuclear structure, and it can provide further constrain on the nuclear structure in heavy-ion collisions.

V. ACKNOWLEDGEMENTS

We thank Jianing Dong for maintaining the high-quality performance of the computer facility. M. Nie is supported by the National Natural Science Foundation of China under Grants 12105156, project ZR2021QA084 supported by Shandong Provincial Natural Science Foundation

and the Fundamental Research Funds of Shandong University. L. Yi is supported by National Natural Science Foundation of China un-

der Grants 11890710 and 11890713. C. Zhang and J. Jia is supported by DOE Award No. DEFG0287ER40331.

-
- [1] J.-Y. Ollitrault, *Phys. Rev. D* **46**, 229 (1992).
- [2] J. Adams *et al.* (STAR), *Nucl. Phys. A* **757**, 102 (2005), [arXiv:nucl-ex/0501009](#) .
- [3] K. Adcox *et al.* (PHENIX), *Nucl. Phys. A* **757**, 184 (2005), [arXiv:nucl-ex/0410003](#) .
- [4] B. Muller, J. Schukraft, and B. Wyslouch, *Ann. Rev. Nucl. Part. Sci.* **62**, 361 (2012), [arXiv:1202.3233 \[hep-ex\]](#) .
- [5] S. Voloshin and Y. Zhang, *Z. Phys. C* **70**, 665 (1996), [arXiv:hep-ph/9407282](#) .
- [6] B. Alver and G. Roland, *Phys. Rev. C* **81**, 054905 (2010), [Erratum: *Phys. Rev. C* **82**, 039903 (2010)], [arXiv:1003.0194 \[nucl-th\]](#) .
- [7] J. E. Bernhard, J. S. Moreland, S. A. Bass, J. Liu, and U. Heinz, *Phys. Rev. C* **94**, 024907 (2016), [arXiv:1605.03954 \[nucl-th\]](#) .
- [8] G. Nijs and W. van der Schee, (2022), [arXiv:2206.13522 \[nucl-th\]](#) .
- [9] D. Everett *et al.* (JETSCAPE), (2020), [arXiv:2011.01430 \[hep-ph\]](#) .
- [10] P. Bozek, W. Broniowski, and J. Moreira, *Phys. Rev. C* **83**, 034911 (2011), [arXiv:1011.3354 \[nucl-th\]](#) .
- [11] A. Bzdak and D. Teaney, *Phys. Rev. C* **87**, 024906 (2013), [arXiv:1210.1965 \[nucl-th\]](#) .
- [12] K. Xiao, F. Liu, and F. Wang, *Phys. Rev. C* **87**, 011901 (2013), [arXiv:1208.1195 \[nucl-th\]](#) .
- [13] P. Huo, J. Jia, and S. Mohapatra, *Phys. Rev. C* **90**, 024910 (2014), [arXiv:1311.7091 \[nucl-ex\]](#) .
- [14] J. Jia and P. Huo, *Phys. Rev. C* **90**, 034915 (2014), [arXiv:1403.6077 \[nucl-th\]](#) .
- [15] V. Khachatryan *et al.* (CMS), *Phys. Rev. C* **92**, 034911 (2015), [arXiv:1503.01692 \[nucl-ex\]](#) .
- [16] M. Aaboud *et al.* (ATLAS), *Eur. Phys. J. C* **78**, 142 (2018), [arXiv:1709.02301 \[nucl-ex\]](#) .
- [17] G. Aad *et al.* (ATLAS), *Phys. Rev. Lett.* **126**, 122301 (2021), [arXiv:2001.04201 \[nucl-ex\]](#) .
- [18] M. Nie (STAR), *Nucl. Phys. A* **982**, 403 (2019).
- [19] G. Denicol, A. Monnai, and B. Schenke, *Phys. Rev. Lett.* **116**, 212301 (2016), [arXiv:1512.01538 \[nucl-th\]](#) .
- [20] P. Bozek and W. Broniowski, *Phys. Lett. B* **752**, 206 (2016), [arXiv:1506.02817 \[nucl-th\]](#) .
- [21] P. Bożek, W. Broniowski, and A. Olszewski, *Phys. Rev. C* **91**, 054912 (2015), [arXiv:1503.07425 \[nucl-th\]](#) .
- [22] L.-G. Pang, G.-Y. Qin, V. Roy, X.-N. Wang, and G.-L. Ma, *Phys. Rev. C* **91**, 044904 (2015), [arXiv:1410.8690 \[nucl-th\]](#) .
- [23] L.-G. Pang, H. Petersen, G.-Y. Qin, V. Roy, and X.-N. Wang, *Eur. Phys. J. A* **52**, 97 (2016), [arXiv:1511.04131 \[nucl-th\]](#) .
- [24] X.-Y. Wu, L.-G. Pang, G.-Y. Qin, and X.-N. Wang, *Phys. Rev. C* **98**, 024913 (2018), [arXiv:1805.03762 \[nucl-th\]](#) .
- [25] L.-G. Pang, H. Petersen, and X.-N. Wang, *Phys. Rev. C* **97**, 064918 (2018), [arXiv:1802.04449 \[nucl-th\]](#) .
- [26] J. Jia, *Phys. Rev. C* **105**, 014905 (2022), [arXiv:2106.08768 \[nucl-th\]](#) .
- [27] G. Giacalone, J. Jia, and C. Zhang, *Phys. Rev. Lett.* **127**, 242301 (2021), [arXiv:2105.01638 \[nucl-th\]](#) .
- [28] J. Jia and C.-J. Zhang, (2021), [arXiv:2111.15559 \[nucl-th\]](#) .
- [29] M. Abdallah *et al.* (STAR), *Phys. Rev. C* **105**, 014901 (2022), [arXiv:2109.00131 \[nucl-ex\]](#) .
- [30] G.-L. Ma and Z.-W. Lin, *Phys. Rev. C* **93**, 054911 (2016), [arXiv:1601.08160 \[nucl-th\]](#) .
- [31] Y. He and Z.-W. Lin, *Eur. Phys. J. A* **56**, 123 (2020), [arXiv:2004.06385 \[hep-ph\]](#) .
- [32] X.-N. Wang and M. Gyulassy, *Phys. Rev. D* **44**, 3501 (1991).
- [33] B. Zhang, *Comput. Phys. Commun.* **109**, 193 (1998), [arXiv:nucl-th/9709009](#) .
- [34] B.-A. Li and C. M. Ko, *Phys. Rev. C* **52**, 2037 (1995), [arXiv:nucl-th/9505016](#) .
- [35] Z.-W. Lin, C. M. Ko, B.-A. Li, B. Zhang, and S. Pal, *Phys. Rev. C* **72**, 064901 (2005), [arXiv:nucl-th/0411110](#) .
- [36] W.-T. Deng, X.-G. Huang, G.-L. Ma, and G. Wang, *Phys. Rev. C* **94**, 041901 (2016), [arXiv:1607.04697 \[nucl-th\]](#) .
- [37] C. Zhang and J. Jia, *Phys. Rev. Lett.* **128**, 022301 (2022), [arXiv:2109.01631 \[nucl-th\]](#) .
- [38] H. Li, H.-j. Xu, Y. Zhou, X. Wang, J. Zhao, L.-W. Chen, and F. Wang, *Phys. Rev. Lett.* **125**, 222301 (2020), [arXiv:1910.06170 \[nucl-th\]](#) .
- [39] H.-j. Xu, H. Li, X. Wang, C. Shen, and F. Wang, *Phys. Lett. B* **819**, 136453 (2021), [arXiv:2103.05595 \[nucl-th\]](#) .
- [40] C. Zhang, S. Bhatta, and J. Jia, (2022), [arXiv:2206.01943 \[nucl-th\]](#) .
- [41] Gaoguo Yan, “Probing initial and final state effects of heavy-ion collisions with star experiment,” <https://indico.cern.ch/event/895086/contributions/4724927> (2022).